Surface-induced intramolecular electron transfer in multi-centre redox metalloproteins: the di-haem protein cytochrome c_4 in homogeneous solution and at electrochemical surfaces

2008 J. Phys.: Condens. Matter 20 374124

(http://iopscience.iop.org/0953-8984/20/37/374124)

IOP PUBLISHING JOURNAL OF PHYSICS: CONDENSED MATTER

J. Phys.: Condens. Matter **20** (2008) 374124 (7pp) doi:10.1088/0953-8984/20/37/374124

Surface-induced intramolecular electron transfer in multi-centre redox metalloproteins: the di-haem protein cytochrome c_4 in homogeneous solution and at electrochemical surfaces

Qijin Chi[1], Jingdong Zhang[1], Palle S Jensen[1], Renat R Nazmudtinov[2] and Jens Ulstrup[1]

[1] Department of Chemistry, Technical University of Denmark, Building 207, DK-2800 Kongens Lyngby, Denmark

[2] Kazan State Technological University, 420015 Kazan, Republic of Tatarstan, Russia

Received 6 February 2008
Published 26 August 2008
Online at stacks.iop.org/JPhysCM/20/374124

Abstract

Intramolecular electron transfer (ET) between transition metal centres is a core feature of biological ET and redox enzyme function. The number of microscopic redox potentials and ET rate constants is, however, mostly prohibitive for experimental mapping, but two-centre proteins offer simple enough communication networks for complete mapping to be within reach. At the same time, multi-centre redox proteins operate in a membrane environment where conformational dynamics and ET patterns are quite different from the conditions in a homogeneous solution.

The bacterial respiratory di-haem protein *Pseudomonas stutzeri* cytochrome c_4 offers a prototype target for environmental gating of intra-haem ET. ET between *P. stutzeri* cyt c_4 and small molecular reaction partners in solution appears completely dominated by *inter*molecular ET of each haem group/protein domain, with no competing *intra*-haem ET, for which accompanying propionate-mediated proton transfer is a further barrier. The protein can, however, be immobilized on single-crystal, modified Au(111) electrode surfaces with either the low-potential N terminal or the high-potential C terminal domain facing the surface, clearly with fast *intra*molecular ET as a key feature in the electrochemical two-ET process. This dual behaviour suggests a pattern for multi-centre redox metalloprotein function. In a homogeneous solution, which is not the natural environment of cyt c_4, the two haem group domains operate largely independently with conformations prohibitive for intramolecular ET. Binding to a membrane or electrochemical surface, however, triggers conformational opening of intramolecular ET channels.

The haem group orientation in *P. stutzeri* cyt c_4 is finally noted to offer a case for orientation dependent electronic rectification between a substrate and a tip in electrochemical *in situ* scanning tunnelling microscopy or nanoscale electrode configurations.

1. Introduction

The core function in biological electron transfer (ET) and catalytic and transport functions is controlled by metalloproteins with several transition metal centres. The photosynthetic reaction centres [1, 2], redox protein complexes such as cytochrome *c* oxidase [3, 4] and nitrogenase [5, 6], and haemoglobin [7] are examples. In addition to direct ET between the metal centres, mutual 'cooperativity' is an important issue. This notion refers to the fact that

injection or extraction of an electron from a given centre or binding of a dioxygen molecule to a given haem group in haemoglobin affects all the microscopic redox potentials, intramolecular ET rate constants and dioxygen binding constants of the other centres. The communication among the centres can be electrostatic, or more subtle protein conformational interactions via the protein structure. The latter is strikingly represented by the cooperative dioxygen transport of haemoglobin [7] and by the microscopic redox potential pattern of the four-haem redox metalloprotein cyt c_3 [8, 9].

The number of all the microscopic electronic interactions in multi-centre redox proteins is mostly prohibitive for complete mapping of their microscopic thermodynamics and reactivity. *Two-centre* redox metalloproteins, however, offer the merits of representing prototype multi-centre redox metalloproteins, at the same time with a simple enough electronic communication network for complete mapping to be within reach. The copper nitrite reductases [10, 11], some haem peroxidases [12, 13], and the bacterial respiratory classes of haem group cyt *cd*'s [14] and cyt c_4's [15] are such examples. The metal centres are here close enough that charge injection at one centre would affect the other centre and that subtle environmentally controlled communication between the centres becomes a crucial part of the overall operation of the proteins.

With a view to illuminating electronic interactions among the metal centres in multi-centre redox metalloproteins, we address here ET patterns of the two-centre haem group protein cyt c_4 both in homogeneous solution and at electrochemical interfaces. Comprehensive data offer, first, a coherent view of the molecular and electronic protein structure. Other data for the ET reactions of the protein with molecular reaction partners in homogeneous solution [16–19] and voltammetric data [20] particularly in the immobilized state on well-defined (single-crystal, atomically planar) electrochemical surfaces [21] are, however, indicative of quite different ET patterns in these two different microenvironments. In particular the roles of intramolecular ET between the two haem groups in overall two-electron protein oxidation and reduction appears quite different. *Intra*molecular ET thus seems largely outcompeted by *inter*molecular ET in homogeneous solution [16–19]. On the other hand, fast intramolecular ET is a conspicuous feature of the protein in the well-defined electrochemical interfacial environments [20, 21].

We offer here an analysis of the electronic coupling in the long-range (19.1 Å) intramolecular ET process between the two haem groups in *P. stutzeri* cyt c_4. In a crude superexchange view the coupling is hypersensitive to the choice of energetic and electronic coupling parameters. This reflects equally strong sensitivity of the electronic coupling to environmental configurational fluctuations particularly in the translational and deformational haem group motion around a propionate hydrogen bond contact between the haem groups. The hydrogen bond contact is thus hypersensitive to environmental configurational fluctuational effects and may even come to constitute an environmentally gated 'on–off' control mechanism. These observations add insight to the understanding of the way that multi-centre redox metalloproteins work in different homogeneous, membrane, and interfacial electrochemical environments. This also points to features of functional triggering when a composite multi-centre redox metalloprotein is brought from a 'resting' solute state to an active functional membrane-bound state.

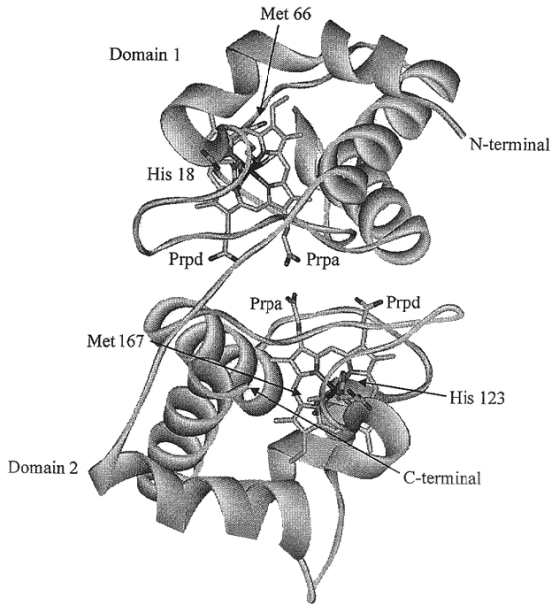

Figure 1. Three-dimensional structure of *P. stutzeri* cyt c_4. The N and C terminal domains, the linking peptide, the haem groups, and the propionate hydrogen bond contacts are shown. Coordinates from [22], PDB code 1EPT. Graphics in Molscript [26].

2. Structural properties, and homogeneous and electrochemical processes of cyt c_4

2.1. Structural, thermodynamic and spectral properties of P. stutzeri cytochrome c_4

We focus on cyt c_4 from the bacterium *Pseudomonas stutzeri* [15]. Three-dimensional structures [22], thermodynamic [15, 17, 20, 21] and folding properties [23], spectral properties [15, 17, 24, 25], data for ET kinetics in homogeneous solution [16–19], voltammetric data [20, 21], and continuum electrostatic computations combined with Monte Carlo sampling of the protein dynamics [15, 25] are available for this two-centre redox metalloprotein. The following structural properties are particularly important:

- The 190-residue protein is organized in two almost equal-size globular domains, each with a haem group and connected by a 12-residue peptide chain; figure 1 [22]. α-helices are dominating secondary structure elements. The sequence homology and structural symmetry of the two domains have been mapped [22]. A hydrogen bond network involving corresponding domain residues (Tyr39/145, Arg61/158, Lys42/148, Asp46/152) is present in the inter-domain region. The protein is strongly dipolar with negative excess charge of the N terminal domain and positive excess charge of the C terminal domain; figure 2

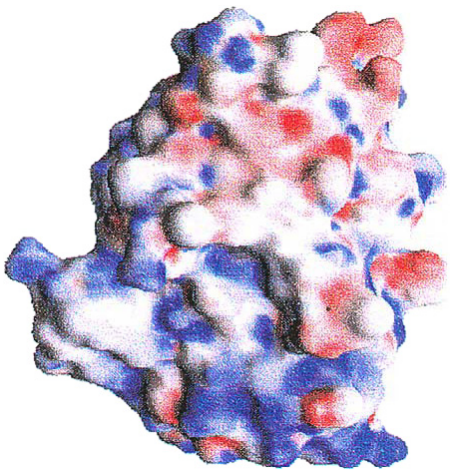

Figure 2. Surface charge distribution of *P. stutzeri* cyt c_4. Red and blue show negative (N terminal domain) and positive (C terminal domain) charge distributions, respectively. Data from [22, 25].

[22, 25]. This has implications for the thermodynamic and kinetic properties of the protein as well as for the overall naturally expected protein function; cf below.

- The haem groups are axially coordinated to histidine (His18/123) and methionine (Met66/167) and further linked to the protein by thioether bonds. Small but functionally important differences between the axial coordinations in the two domains are notable [22]. A structural feature of crucial importance for inter-haem ET is that the haem groups are strongly hydrogen bonded to each other by two haem group propionates; figure 3 [22]. This almost certainly implies that intramolecular ET between the haem groups is accompanied by proton transfer between the propionate carboxylate groups. Such a contact would invoke exceeding ET sensitivity to conformational fluctuations in the protein and solvent environment. The Fe–Fe distance is 19.1 Å with a tilt angle between the haem planes of 30°. This motif is also encountered in other di-haem proteins [22, 27, 28].
- Redox potentials have been determined by reversible ET kinetics [17] and cyclic voltammetry [20, 21]. The macroscopic values ≈240 mV and ≈330 mV (SHE) represent the N and C terminal haem group, respectively. This follows expectations from the negative and positive electrostatic charges of the two domains but the small structural differences in axial Met coordination would also contribute to the difference. Microscopic redox potentials dominated by electrostatic interactions ('negative cooperativity') were determined from the ET kinetics of the two-ET processes of *P. stutzeri* cyt c_4 in homogeneous solution [17]; cf below. Selective thermodynamic domain stability is also reflected in chemically and thermally induced unfolding. Guanidium-induced unfolding shows a two-step unfolding process caused by sequential unfolding first of the N and then of the C terminal domain [23]. Differential domain stability is supported by other data, particularly resonance Raman spectroscopy [24].

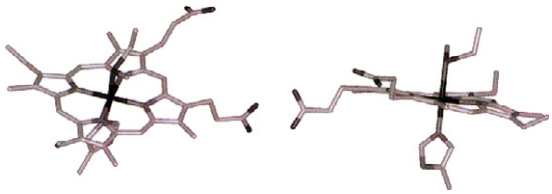

Figure 3. The haem groups with axial ligands and the propionate hydrogen bond contact in *P. stutzeri* cyt c_4.

- UV/visible spectra of oxidized and reduced *P. stutzeri* cyt c_4 show the α, β and Soret features as well as a 701 nm band (oxidized form) [17, 23] characteristic of His/Met coordinated class I cyt *c*'s [29]. A 620 nm high-spin fingerprint band of oxidized cyt c_4 is also observed. The 620 and 701 nm bands show almost exactly opposite temperature dependence [15, 30]. The former gradually disappears when cryogenic temperatures are approached whereas the latter builds up. This is strongly indicative of a temperature dependent high-spin/low-spin equilibrium where the former dominates completely at low temperatures. NMR, EPR and resonance Raman spectroscopy support this view. NMR spectral titration identify the low-potential, partly high-spin component specifically with the N terminal haem group [15] supported by high-spin marker resonance Raman bands [24]. Overall the structural, thermodynamic and spectral data support a coherent view of cyt c_4 with a low-spin C terminal haem group in both oxidation states and a more open pocket N terminal domain haem group with a low-spin reduced form and a temperature dependent low-spin/high-spin equilibrium of the N terminal domain in the oxidized state.

2.2. ET between P. stutzeri cyt c_4 and reaction partners in homogeneous solution

ET reactions of *P. stutzeri* cyt c_4 with the inorganic reaction partners $[Co(terpy)_2]^{2+/3+}$ and $[Co(bipy)_3]^{2+/3+}$ (bipy = 2,2′-bipyridine; terpy = 2,2′,2′-terpyridine) [17, 18] and with flavin and methylviologen radicals [19] have been studied. The ET reactions between cyt c_4 and the inorganic reaction partners (1–100 ms time range) show two or three kinetic phases dominated by parallel electron exchange at both haem groups. Microscopic reduction potentials reflecting electrostatic interactions could be obtained, as noted [17]. There was no conclusive kinetic indication of *intra*molecular ET between the haem groups. Intramolecular ET would, on the other hand, have to compete with quite fast (millisecond range) *inter*molecular ET at the two haem groups. A free energy plot showed an apparent reorganization free energy significantly larger than for single-haem horse heart cyt *c* (1.1 eV versus 0.8 eV) [19]. This difference could be rooted in the high-spin/low-spin equilibrium of cyt c_4 which would contribute to the intramolecular nuclear reorganization compared with cyt *c* with pure low-spin configurations in both oxidation states.

2.3. Voltammetry and intramolecular ET of P. stutzeri cyt c_4

Cyclic voltammetry offers a way of addressing intra-haem ET in *P. stutzeri* cyt c_4 that circumvents competition from intermolecular ET. Data from polycrystalline [20] and particularly new data based on single-crystal Au(111) electrodes [21] modified by self-assembled monolayers of thiol-based promoter molecules with positively (the ammonium group) and negatively charged functional groups (the carboxylate group) orient *P. stutzeri* cyt c_4 on the electrode surface in orientations where the negatively (N terminal, low-potential haem group) and positively charged (C terminal, high-potential haem group) domain, respectively, face the electrode surface. Two-electron interfacial oxidation or reduction is then *only* possible by interfacial ET between the electrode surface and the adjacent haem group followed by oxidation or reduction of the remote haem group solely via intramolecular ET between the haem groups. Interfacial electrochemical ET therefore follows a pattern quite different from that of ET of cyt c_4 in homogeneous solution.

Cyclic voltammograms show intriguing asymmetry that entirely supports this view. If for example, the high-potential haem group is adjacent to the electrode surface, then this group is first reduced in a cathodic scan, and this is followed by reduction of the remote low-potential haem group at the lower potential of this group. *Two one-electron* peaks are therefore expected. In the reverse scan the low-potential remote haem group cannot, however, be re-oxidized until the higher potential is reached where the adjacent high-potential haem group is re-oxidized. *A single two-electron* peak is therefore expected. A reverse pattern of a single two-electron cathodic peak and two one-electron anodic peaks is expected when the low-potential haem group is adjacent to the electrode surface. Details of these patterns offer a route to the intramolecular ET rate constants.

Cyclic voltammetry of *P. stutzeri* cyt c_4 particularly on variably modified single-crystal Au(111) electrode surfaces does indeed show sharp peaks that accord entirely with these expectations. Data analysis based on numerically computed voltammograms [20, 21] gives, notably, *large* values of the intramolecular ET rate constants, i.e. around 10^2–10^3 s^{-1} for the $C_{terminal} \rightarrow N_{terminal}$ ET process and $\approx 10^4$ s^{-1} for the $N_{terminal} \rightarrow C_{terminal}$ ET process (the two rate constants are related by the equilibrium redox potential difference of the haem groups). If values in these ranges were to apply to *P. stutzeri* cyt c_4 in homogeneous solution, they would have been disclosed as a fast *intra*molecular electronic equilibrium between the two haem groups compared with slower *inter*molecular ET rates [17]. As noted, this is not what was observed.

A preliminary conclusion is that the intramolecular ET rate constants are indeed quite different in the two environments, i.e. much slower in homogeneous solution than at the electrochemical interface. It is as if binding to the electrode surface modified by 'soft' molecular monolayers triggers an intramolecular ET channel between the two haem groups. This raises issues about the nature of the ET channel along the propionate groups via the hydrogen bond contact (figure 3) and the sensitivity of the electronic tunnelling factor to environmental configurational fluctuations and gating. The most conspicuous deformational motion is the tilt angle between the two haem groups and the hydrogen bond contact between the propionate groups. The latter would not only affect the ET process but also strongly affect the proton transfer step that must accompany the ET process [25]. We address these issues in the next section using a simple theoretical framework. The crucial ET parameter is the electronic transmission coefficient and the accompanying controlling proton tunnelling factor. Even these simple views disclose important issues concerning the adiabatic or diabatic nature of the ET process and the roles of the gating nuclear modes and the proton transfer step. These views thus hold obvious first clues to the somewhat composite nature of the intramolecular ET process and to the implications of binding of the protein to natural surface environments for *P. stutzeri* cyt c_4 operation. We shall substantiate this view in a forthcoming communication by means of detailed density functional calculations based on the core haem groups and their axial ligands, as well as the propionate-mediated hydrogen bond contact between the haem groups.

3. Intramolecular ET between the cyt c_4 haem groups and environmental configurational fluctuations and gating—a simple view

3.1. Rate constants and electronic transmission coefficients based on directional tunnelling

We use the following rate constant form (s^{-1}) for the intramolecular, inter-haem ET process [31, 32]:

$$W(s^{-1}) = \kappa_{el}\frac{\omega_{eff}}{2\pi}\exp\left[-\frac{(E_r + \Delta G^0)^2}{4E_r k_B T}\right]. \qquad (1)$$

ΔG^0 is the reaction free energy (driving force), E_r the total nuclear reorganization free energy, ω_{eff} the effective vibrational frequency and κ_{el} the electronic transmission coefficient. k_B is Boltzmann's constant and T the temperature. In the following we let $\Delta G^0 \approx 0$ as $|\Delta G^0| \ll E_r$ from the haem group redox potential difference. Equation (1) is then recast as

$$W(s^{-1}) \approx (T_{DA})^2\sqrt{\frac{\pi}{E_r k_B T\hbar^2}}\exp\left(-\frac{E_r}{4k_B T}\right);$$
$$\kappa_{el} = (T_{DA})^2\sqrt{\frac{4\pi^3}{E_r k_B T\hbar^2\omega_{eff}^2}}. \qquad (2)$$

Subject to $\kappa_{el} \ll 1$, i.e. in the diabatic limit of weak electronic donor–acceptor coupling, T_{DA} is the electron exchange factor and $\hbar$ Planck's constant divided by 2π. $\kappa_{el} \rightarrow 1$ in the opposite adiabatic limit of strong coupling.

We invoke the following crude but useful estimate of T_{DA} [32]:

$$T_{DA} \approx \frac{\beta_D\beta_A}{\beta}\left(\frac{\beta}{\Delta}\right)^M \qquad (3)$$

where β is the average electron exchange coupling between nearest neighbour bridge groups along the tunnelling route

between the haem groups. β_D and β_A are the exchange couplings between the donor and the acceptor group, respectively, and their nearest intermediate bridge group. Δ is the average energy gap between the donor and bridge groups, and M the number of bridge groups. The choice of intermediate bridge groups is somewhat arbitrary. Bridge groups could be represented either by intermediate atomic [33, 34] or molecular fragment orbitals [32, 35]. We shall take the individual C–C bonds as intermediate states. The hydrogen bond contact should be assigned separate values, β_H and Δ_H, leaving altogether 14 covalent links between the donor and acceptor iron atoms. Taking further $\beta \approx \beta_D \approx \beta_A$, equation (3) gives

$$T_{DA} \approx \beta \left(\frac{\beta}{\Delta}\right)^{14} \left(\frac{\beta_H}{\Delta_H}\right) \tag{4}$$

or for the rate constant and the transmission coefficient

$$W \approx \frac{\beta^2}{\hbar}\sqrt{\frac{\pi}{E_r k_B T}} \left(\frac{\beta}{\Delta}\right)^{28} \left(\frac{\beta_H}{\Delta_H}\right)^2 \exp\left(-\frac{E_r}{4k_B T}\right);$$
$$\kappa_{el} = \frac{\beta^2}{\hbar\omega_{eff}}\sqrt{\frac{4\pi^3}{E_r k_B T}} \left(\frac{\beta}{\Delta}\right)^{28} \left(\frac{\beta_H}{\Delta_H}\right)^2. \tag{5}$$

Appropriate but adequate values for E_r, β and ω_{eff} are $E_r \approx 1$ eV and $\omega_{eff} = 10^{12}$–10^{13} s^{-1}, giving

$$W(\mathrm{s}^{-1}) = 8 \times 10^{11} \beta^2 \left(\frac{\beta}{\Delta}\right)^{28} \left(\frac{\beta_H}{\Delta_H}\right)^2;$$
$$\kappa_{el} \approx (2\text{–}5) \times 10^5 \beta^2 \left(\frac{\beta}{\Delta}\right)^{28} \left(\frac{\beta_H}{\Delta_H}\right)^2. \tag{6}$$

The numerical factors here have little sensitivity to the parameter values. The equivalent form

$$W \approx \frac{\beta^2}{\hbar}\sqrt{\frac{\pi}{E_r k_B T}} \exp\left[-\frac{1}{a}\left(\ln\frac{\Delta}{\beta}\right) R\right] \left(\frac{\beta_H}{\Delta_H}\right)^2 \times \exp\left(-\frac{E_r}{4k_B T}\right) \tag{7}$$

where R is the (conformationally fluctuating) Fe–Fe distance and a the average spatial bridge group extension (C–C bond length) emphasizes the extreme sensitivity of the intramolecular ET rate constant to the electronic parameter combination β/Δ for *long-range* ET, i.e. when $R/a \gg 1$.

A broadly recommended value of β/Δ is $\beta/\Delta = 0.6$ [33, 34]. Taking this value also for β_H/Δ_H gives $W = 1.8 \times 10^5$ s^{-1} for the rate constant and $\kappa_{el} = 0.04$–0.1 for the electronic transmission coefficient. The intramolecular ET process thus belongs to the weakly diabatic regime, leading to intramolecular ET in the sub-millisecond range. Only slightly weaker electronic coupling, however, gives an entirely different behaviour and shifts the ET pattern into the strongly diabatic range with slow intramolecular ET. Taking the slightly smaller value $\beta/\Delta = \beta_H/\Delta_H = 0.4$ thus gives the much smaller values of $W \approx 1$ s^{-1} and $\kappa_{el} = (0.5\text{–}1) \times 10^{-6}$.

The non-covalent protein transfer contact between the propionates would invoke an additional conformationally highly sensitive controlling factor in the inter-haem ET process. Due to the combined diabatic ET and proton tunnelling steps that the process offers, we have an interesting and rare case of totally diabatic proton transfer, as opposed to the much more representative partially or fully adiabatic proton transfer processes in the sense discussed elsewhere [31, 32]. β_H/Δ_H can be represented as [31, 32]

$$\left(\frac{\beta_H}{\Delta_H}\right)^2 = \exp\left(-\frac{m_H \Omega_H (\Delta R_H)^2}{2\hbar}\right) \tag{8}$$

where m_H is the proton mass, Ω_H the proton stretching vibrational frequency and ΔR_H the proton transfer distance. Equation (8) rests on a view of proton motion in a pair of displaced harmonic potential surfaces. The crystallographic proton transfer distance in the *P. stutzeri* cyt c_4 structure is 0.6 Å but fluctuational gating would modify (reduce) this distance to a smaller value at the non-equilibrium configuration at the moment of electron and proton transfer [31, 32, 36].

Proton transfer along an O–H stretching mode over the equilibrium proton transfer distance of 0.6 Å in the unperturbed double-well potential would reduce the rate constant by a factor of 4×10^{-8} solely in the transmission coefficient. As noted, haem group configurational fluctuations would both reduce this distance and strongly distort the potential surfaces towards lower effective proton vibrational frequencies. The scaling factor is 7×10^{-6}, 6×10^{-4} and 1.5×10^{-2} for the smaller formal values of ΔR_H of 0.5 Å, 0.4 Å, and 0.3 Å, respectively. The corresponding rate constants would be ≈ 1 s^{-1}, 10^2 s^{-1} and 2.5×10^3 s^{-1} for $\Delta R_H = 0.5$ Å, 0.4 Å and 0.3 Å, respectively, when $\beta/\Delta = 0.6$ and (6–8) $\times 10^{-6}$ s^{-1}, (5–7) $\times 10^{-4}$ s^{-1} and (1–2) $\times 10^{-2}$ s^{-1} when $\beta/\Delta = 0.4$. As noted, the strong hydrogen bond contact reduces the vibrational frequencies of the proton relative to the unperturbed value of 6×10^{14} s^{-1} used in the estimates. The real proton transfer attenuation of the ET process may thus be significantly smaller but is still highly sensitive to environmental gating such as translational or deformational motion of the two haem groups or protein domains.

3.2. Conclusions regarding intramolecular ET operation of *P. stutzeri* cyt c_4

The ET patterns as reflected in the rate constant, and the electronic and proton tunnelling factors, emerge as hypersensitive to the electronic coupling parameters β and Δ and the dynamic proton transfer properties. This observation applies to inter-haem group configurational fluctuations and to widely different intramolecular ET rate constants of *P. stutzeri* cyt c_4 in bulk- and surface-confined environments. The rate constant and the tunnelling factor estimates thus suggest that the inter-haem ET processes (forward and reverse) in *P. stutzeri* cyt c_4 belong to the diabatic limit of weak electronic inter-haem coupling. Even small variations of β/Δ, however, change the rate constant by many orders of magnitude. Variations in the environmental reorganization free energy E_r are much less important. Such variations in the tunnelling parameters can be induced by conformational fluctuations or electronic gating in the inter-haem group dynamics. The observed sensitivity

of the superexchange tunnelling factor then strongly implies that conformational gating is crucial in the intramolecular ET pattern. The effect of a gating mode on the proton transfer step adds no less strongly to this sensitivity, constituting perhaps even an intramolecular ET 'switch' as the inter-haem hydrogen bond may well be broken or re-established along with the environmental gating mode fluctuations.

The intramolecular ET behaviours of *P. stutzeri* cyt c_4 appear widely different for homogeneous solution and at electrochemical interfaces. No real evidence of intramolecular ET in intermediate (i.e. competitive with *inter*molecular ET) or fast time ranges (intramolecular ET equilibrium) could be detected for the ET processes in homogeneous solution. On the other hand, the voltammetric pattern of *P. stutzeri* cyt c_4 points strongly to fast (millisecond to sub-millisecond time ranges) intramolecular ET. While at first puzzling, the extreme sensitivity of the ET process and the inter-haem group hydrogen bond contact to environmental gating offers a clue to this conspicuously different intramolecular ET behaviour. The local microenvironment in the isotropic homogeneous solution differs in important respects from the inhomogeneous anisotropic ET environments at the modified electrochemical interface. There is also here no competition from *inter*molecular ET channels. It could be conjectured that the latter reflects the membrane environments as the natural working environment of *P. stutzeri* cyt c_4. An interesting scenario could then be that there is no biological need for intramolecular ET of *P. stutzeri* cyt c_4 when 'stored' in bulk solution where the two domains behave as largely independent entities and the key (intramolecular ET) protein function is inoperative. Binding of *P. stutzeri* cyt c_4 in its functional membrane environment, however, triggers conformational inter-domain gating that opens a favourable intramolecular long-range ET channel. Such a view is in keeping with the natural role of *P. stutzeri* cyt c_4 as part of a respiratory membrane-bound electron transport complex.

We have initiated a programme to explore the electronic coupling using large-scale structure dependent density functional-based computations to address the electronic structure of the di-haem core of *P. stutzeri* cyt c_4 in greater detail than in the operational but crude formalism presently used, equations (4)–(8). Local and bulk viscosity effects, i.e. ultimately environmental nuclear relaxation effects, could offer other clues. Relaxation effects are associated with the adiabatic limit of strong donor–acceptor electronic interaction. The electronic coupling estimates above, however, suggest that the weak coupling diabatic limit of the intramolecular ET process prevails. Together with the small intramolecular ET rate constants in solution, viscosity effects in homogeneous solution would therefore primarily reflect relaxation features of the *inter*molecular ET processes. Viscosity features might, however, be expected for the intramolecular ET process in the electrochemical environment if gating in the sense noted is a controlling factor. Studies of the viscosity dependence of the monolayer voltammetric patterns of *P. stutzeri* cyt c_4 could therefore hold other clues to gating in the intramolecular ET process.

By its dipolar nature and the controlled dual orientation on appropriately modified well-defined electrode surfaces, *P. stutzeri* cyt c_4 offers, finally, a new kind of target metalloprotein for *in situ* approaches to *single-molecule* bioelectronics directly in aqueous biological media [37–43]. Electronic conductivity and *in situ* scanning tunnelling microscopic image patterns in such configurations would offer new insight into the intramolecular, inter-haem ET process. The di-haem nature of the protein is, for example, expected to display interfacial bioelectronic tunnelling current rectification for which theoretical frameworks are available [44]. The rectification features would moreover take different forms in the two protein surface orientations that we can now control. Studies along these lines have been initiated [21].

Acknowledgment

Financial support from the Danish Research Council for Technology and Production Sciences (Grant No. 07-021510) is acknowledged.

References

[1] Michel-Beyerle M E and Small G J (ed) 1995 Chemical physics special issue on photosynthesis and the bacterial reaction center *Chem. Phys.* **197** 223–472
[2] Chuang J I, Boxer S G, Holten D and Kirmaier C 2007 *Biochemistry* **45** 3845 and references there
[3] Yoshikawa S, Shinzawa-Itoh K, Yamashita E and Tsukihara T 2001 *Handbook of Metalloproteins* vol 1, ed A Messerschmidt, R Huber, T Poulos and K Wieghardt (Chichester: Wiley) p 348
[4] Gray H B and Winkler J R 2005 *Proc. Natl Acad. Sci. USA* **102** 3534 and references there
[5] Schmid B, Chiu H-J, Ramakrishnan V, Howard J B and Rees D C 2001 *Handbook of Metalloproteins* vol 2, ed A Messerschmidt, R Huber, T Poulos and K Wieghardt (Chichester: Wiley) p 1025
[6] Rees D C 2002 *Annu. Rev. Biochem.* **71** 221
[7] Paoli M and Nagai K 2001 *Handbook of Metalloproteins* vol 1, ed A Messerschmidt, R Huber, T Poulos and K Wieghardt (Chichester: Wiley) p 16
[8] Coutinho I B and Xavier A V 1994 *Methods Enzymol.* **243** 119
[9] Paquete C M, Turner D L, Louro R O, Xavier A V and Caterino T 2007 *Biochim. Biophys. Acta—Bioenerg.* **1767** 1169
[10] Adman E T and Murphy E P 2001 *Handbook of Metalloproteins* vol 2, ed A Messerschmidt, R Huber, T Poulos and K Wieghardt (Chichester: Wiley) p 1381
[11] Welinder A C, Zhang J, Hansen A G, Moth-Poulsen K, Christensen H E M, Kuznetsov A M, Bjørnholm T and Ulstrup J 2007 *Z. Phys. Chem.* **221** 1343 and references there
[12] Ellfolk N, Rönnberg M, Aasa R, Andréasson L-E and Vänngård T 1983 *Biochim. Biophys. Acta* **743** 23
[13] Villalain J, Moura I, Liu M C, Payne W J, LeGall J, Xavier A V and Moura J J G 1984 *Eur. J. Biochem.* **141** 305
[14] Farver O, Kroneck P M H, Zumft W G and Pecht I 2003 *Proc. Natl Acad. Sci. USA* **100** 7622
[15] Andersen N H, Christensen H E M, Iversen G, Nørgaard A, Scharnagle C, Thuesen M H and Ulstrup J 2001 *Handbook of Metalloproteins* vol 1, ed A Messerschmidt, R Huber, T Poulos and K Wieghardt (Chichester: Wiley) p 100
[16] Gadsby P M A, Hartskorn R T, Moura J J G, Sinclair-Day J D, Sykes A G and Thompson A J 1989 *Biochim. Biophys. Acta* **994** 37
[17] Conrad L S, Karlsson J-J and Ulstrup J 1995 *Eur. J. Biochem.* **231** 133

[18] Karlsson J-J, Rostrup T E and Ulstrup J 1996 *Acta Chem. Scand.* **50** 284
[19] Andersen N H, Hervás M, Navarro J A, De la Rosa M A and Ulstrup J 1998 *Inorg. Chim. Acta* **272** 109
[20] Karlsson J-J, Nielsen M F, Thuesen M H and Ulstrup J 1997 *J. Phys. Chem.* B **101** 2430
[21] Chi Q, Zhang J, Jensen P S and Ulstrup J 2008 in preparation
[22] Kadziola A and Larsen S 1997 *Structure* **5** 203
[23] Andersen N H, Nørgaard A, Jensen T J and Ulstrup J 2002 *J. Inorg. Biochem.* **88** 316
[24] Nissum M, Karlsson J-J, Ulstrup J, Jensen P W and Smulevich G 1997 *J. Biol. Inorg. Chem.* **2** 302
[25] Iversen G 1998 Molecular electrostatics and electron tunnelling in metalloproteins *PhD Diss.* Technical University of Denmark, Copenhagen
[26] Kraulis P 1991 *J. Appl. Crystallogr.* **24** 946
[27] Van Beeumen J J, Demol H, Samyn B, Bartsch R G, Meyer T E, Dolata M M and Cusanovich M A 1991 *J. Biol. Chem.* **266** 12921
[28] Chen Z, Koh M, Vandriessche G, Van Beeumen J J, Bartsch R G, Meyer T E, Cusanovich M A and Mathews F S 1994 *Science* **266** 430
[29] Moore G R and Pettigrew G W 1990 *Cytochromes c. Evolutionary, Structural and Physicochemical Aspects* (Berlin: Springer)
[30] Andersen N H 2000 Electronic properties of two-centre iron proteins *PhD Diss.* Technical University of Denmark, Copenhagen
[31] Kuznetsov A M 1995 *Charge Transfer in Physics, Chemistry and Biology* (Reading, MA: Gordon and Breach)
[32] Kuznetsov A M and Ulstrup J 1999 *Electron Transfer in Chemistry and Biology. An Introduction to the Theory* (Chichester: Wiley)
[33] Beratan D N, Betts J N and Onuchic J N 1991 *Science* **252** 1285
[34] Gray H B and Winkler J R 2003 *Q. Rev. Biophys.* **36** 341
Hammerich O and Ulstrup J (ed) 2008 *Bioinorganic Electrochemistry* (Dordrecht: Springer)
[35] Christensen H E M, Conrad L S, Mikkelsen K V, Nielsen M K and Ulstrup J 1990 *Inorg. Chem.* **29** 2808
[36] Kuznetsov A M and Ulstrup J 1999 *Can. J. Chem.* **77** 1085
Kuznetsov A M and Ulstrup J 2004 *Russ. J. Electrochem.* **40** 1010
Kohen A and Limbach H-H (ed) 2006 *Isotope Effects in Chemistry and Biology* (Boca Raton, FL: Taylor and Francis) p 691
Kuznetsov A M and Ulstrup J 2004 *Russ. J. Electrochem.* **40** 1000
[37] Chi Q, Zhang J, Nielsen J U, Friis E P, Chorkendorff I, Canters G W, Andersen J E T and Ulstrup J 2000 *J. Am. Chem. Soc.* **122** 4047
Chi Q, Farver O and Ulstrup J 2005 *Proc. Natl Acad. Sci. USA* **102** 16203
[38] Zhang J, Christensen H E M, Ooi B L and Ulstrup J 2004 *Langmuir* **20** 10200
[39] Zhang J, Chi Q, Kuznetsov A M, Hansen A G, Wackerbarth H, Christensen H E M, Andersen J E T and Ulstrup J 2002 *J. Phys. Chem.* B **106** 1131
[40] Zhang J, Welinder A C, Hansen A G, Christensen H E M and Ulstrup J 2003 *J. Phys. Chem.* B **107** 12480
Chi Q, Zhang J, Jensen P S, Christensen H E M and Ulstrup J 2006 *Faraday Discuss.* **131** 181
[41] Zhang J, Chi Q, Albrecht T, Kuznetsov A M, Grubb M, Hansen A G, Wackerbarth H, Welinder A C and Ulstrup J 2005 *Electrochim. Acta* **50** 3143
[42] Alessandrini A, Corni S and Facci P 2006 *Phys. Chem. Chem. Phys.* **8** 4383
[43] Bonanni B, Andolfi L, Bizzarri A R and Cannistraro S 2007 *J. Phys. Chem.* B **111** 5062
[44] Kuznetsov A M and Ulstrup J 2002 *J. Chem. Phys.* **116** 2149